Research in Astron. Astrophys. **2010** Vol. **10** No. **12**, 1287–1297
http://www.raa-journal.org *http://www.iop.org/journals/raa*

Research in Astronomy and Astrophysics

The Galactic halo magnetic field revisited

Xiao-Hui Sun[1,2] and Wolfgang Reich[2]

[1] National Astronomical Observatories, Chinese Academy of Sciences, Beijing 100012, China; *xhsun@nao.cas.cn; xhsun@mpifr-bonn.mpg.de*

[2] Max-Planck-Institut für Radioastronomie, Auf dem Hügel 69, 53121 Bonn, Germany; *wreich@mpifr-bonn.mpg.de*

Received 2010 August 18; accepted 2010 October 21

Abstract Recently, Sun et al. published new Galactic 3D-models of magnetic fields in the disk and halo of the Milky Way and the distribution of cosmic-ray electron density by taking into account the thermal electron density model NE2001 by Cordes & Lazio. The models successfully reproduce observed continuum and polarization all-sky maps and the distribution of rotation measures of extragalactic sources across the sky. However, the model parameters obtained for the Galactic halo, although reproducing the observations, seem physically unreasonable: the magnetic field needs to be significantly stronger in the Galactic halo than in the plane and the cosmic-ray distribution must be truncated at about 1 kpc to avoid excessive synchrotron emission from the halo. The reason for these unrealistic parameters was the low scale-height of the warm thermal gas of about 1 kpc adopted in the NE2001 model. However, this scale-height seemed reasonable and was well studied by numerous investigations. Recently, the scale-height of the warm gas in the Galaxy was revised by Gaensler et al. to about 1.8 kpc, by showing that the 1 kpc scale-height results from a systematic bias in the analysis of pulsar data. This implies a higher thermal electron density in the Galactic halo, which in turn reduces the halo magnetic field strength to account for the observed rotation measures of extragalactic sources. We slightly modified the NE2001 model according to the new scale-height and revised the Sun et al. model parameters accordingly: the strength of the regular halo magnetic field is now 2 μG or lower, and the physically unrealistic cutoff in z for the cosmic-ray electron density is removed. The simulations based on the revised 3D-models reproduce all-sky observations as before.

Key words: ISM: magnetic fields — ISM: structure — radio continuum: ISM

1 INTRODUCTION

It is important to obtain a realistic model of the Galactic magnetic field, cosmic-ray and thermal electron density distribution for the understanding of the physical processes in the magnetized interstellar medium. Relativistic electrons lose their energy in the Galactic magnetic field by polarized synchrotron emission. Synchrotron emission fluctuations are the primary contamination for the analysis of cosmic microwave background observations. The Galactic magnetic field causes deflections of ultrahigh energy cosmic-rays, which must be corrected for to identify their origin. The magnetized thermal interstellar medium generates rotation measures (RMs) in the direction of extragalactic sources, which must be properly subtracted. However, it is very challenging to obtain realistic

Galactic 3D-models because of our position inside of the Galactic disk and the limited number of all-sky surveys at different frequencies needed for this task.

The results from earlier modeling of the Galactic magnetic field, relativistic and thermal electron densities have been reviewed by Sun et al. (2008). Most of the models were only derived from selected data sets and do not agree with other observations. Sun et al. (2008) made the first attempt to establish 3D-emission models (SRWE08 models hereafter) aiming to properly represent all relevant available radio observations, such as RMs of extragalactic sources, and total intensity and polarization all-sky surveys. Jansson et al. (2009) and Jaffe et al. (2010) followed that attempt and additionally invoked a quantitative comparison with the observations. However, Jansson et al. (2009) did not take into account total intensity maps and Jaffe et al. (2010), so far, presented a 2D disk model. Sun et al. (2008) relied on a qualitative comparison between simulations and observations, which seems at the present stage sufficient to constrain 3D models describing global Galactic properties. A quantitative comparison needs to separate local large-scale features and more distant anomalies from the all-sky maps, which is a very ambitious task on its own and beyond our scope.

The SRWE08 models are based on the thermal electron density model NE2001 by Cordes & Lazio (2002, 2003), which uses a scale-height of about 1 kpc. To account for the RMs of extragalactic sources at high latitudes, a strong regular halo magnetic field of up to about 10 μG was required. Subsequently, the cosmic-ray electron density distribution needs to be cut in z[1] at 1 kpc below and above the Galactic plane to avoid excessive polarized emission at high latitudes. However, both the strong halo field and the z-truncation of the cosmic-ray electron density are physically unrealistic. As already argued by Sun et al. (2008), this problem could be solved by increasing the thermal electron density scale-height by a factor of about two. Recently, a scale-height of about 1.8 kpc was derived by Gaensler et al. (2008), which is very close to our prediction. This motivates us to update the SRWE08 models.

The paper is organized as follows: we briefly describe the method and available observations in Section 2, revise the SRWE08 models in Section 3, and summarize our results in Section 4.

2 THE METHOD AND AVAILABLE OBSERVATIONS

We follow the same method to obtain 3D-emission models as already detailed by Sun et al. (2008). The thermal electron density model NE2001 was the basis for the SRWE08 models and needs revision to adapt for the larger scale-height by Gaensler et al. (2008). The thermal electron density $n_{\rm e}$ and the regular magnetic field component $B_{\parallel}$ along the line-of-sight l were obtained from RMs of extragalactic sources, $\mathrm{RM} \sim n_{\rm e} B_{\parallel} l$. The random field and the cosmic-ray electron density were constrained by total intensity and polarization all-sky maps. The Hammurabi code by Waelkens et al. (2009) was used to simulate all-sky emission, which was then compared to the observations. Despite recent efforts, the RMs of extragalactic sources are still sparsely distributed and are likely influenced by local structures on large scales in an unknown way, so that a quantitative χ^2-fit will not determine the halo parameters more reliably than our qualitative approach.

We used RMs from the Canadian Galactic Plane Survey (CGPS, Brown et al. 2003) and the Southern Galactic Plane Survey (SGPS, Brown et al. 2007) to constrain the magnetic field in the Galactic disk. For the halo, previous RM measurements collected by Han et al. (1997) and the Effelsberg L-band RM survey (Han et al. in prep.) were used by Sun et al. (2008). Recently, Taylor et al. (2009) obtained RMs of 37 543 extragalactic sources by re-processing the polarization data from the NVSS survey (Condon et al. 1998). This is the largest RM data set available so far. Mao et al. (2010) pointed out that individual NVSS RMs might have large errors, since they were only derived from two frequencies. NVSS RMs towards the plane are not always reliable because the large RMs there are usually beyond the ambiguity limits as explained by Taylor et al. (2009). However,

[1] The cylindrical coordinate (R, ϕ, z) is defined as: R is the Galactocentric radius, ϕ is the azimuth angle starting from $l = 0^\circ$ and increasing in the counterclockwise direction, and z is the distance to the Galactic plane.

this data set should describe Galactic large-scale structures well beyond the plane. Therefore, we included these RM data to constrain the magnetic field in the halo. The RMs for the region of $100^\circ < l < 120^\circ$ and $-5^\circ < b < 20^\circ$ from the CGPS extension (Brown et al. in prep.) were also used.

The 408 MHz total intensity all-sky survey (Haslam et al. 1982) and the WMAP five-year 22.8 GHz polarization map (Hinshaw et al. 2009) both trace Galactic synchrotron emission and were used to constrain the total magnetic fields and cosmic-ray electron density. The WMAP five-year MEM free-free emission template (Gold et al. 2009) served as a crosscheck for the thermal electron density distribution model.

3 MODELING REVISITED

3.1 Thermal Electron Density

NE2001 is a 3D-model describing the diffuse Galactic thermal gas (Cordes & Lazio 2002, 2003). The thermal electron density distribution consists of several components: a thin disk, a thick disk, spiral arms and, in addition, a large number of thermal source complexes, which is, however, not complete. The ionized gas at high latitudes is primarily attributed to the thick disk component with a scale-height of about 1 kpc and a mid-plane density of about 0.034 cm^{-3}. This scale-height was determined by fitting DM $\sin|b|$ versus $|z|$ of pulsars, which have either measured parallaxes or are associated with globular clusters at known distances. $\mathrm{DM} \sim n_\mathrm{e} l$ is the dispersion measure of a pulsar at a distance l.

The NE2001 model was widely used, although shortcomings were noted soon, such as the decrease of z with pulsar distance (Kramer et al. 2003; Lorimer et al. 2006). Recently, Gaensler et al. (2008) convincingly demonstrated that many DMs of low-latitude pulsars are influenced by local structures such as H II regions along the line-of-sight and derived a scale-height of about 1.8 kpc by including only pulsars at $|b| \geq 40^\circ$. The mid-plane density derived was 0.014 cm^{-3}. Gaensler et al. (2008) also found that the filling factor of the thermal gas, which was not addressed in the NE2001 model, grows exponentially in the range of $0 \leq |z| \leq 1.4$ kpc with a scale-height of 0.7 kpc. This differs from the filling factors obtained by Berkhuijsen et al. (2006) and Berkhuijsen & Müller (2008).

In the following, we modify the NE2001 model by replacing the scale-height and the mid-plane density for the thick disk component by those provided by Gaensler et al. (2008). We investigated the modified NE2001 model by comparing the distances of pulsars estimated from the model by their quoted DMs with that from independent measurements, such as parallax and the associated globular clusters. The up-to-date parallax measurements for pulsars were collected by Verbiest et al. (2010). We obtained DMs of these pulsars from the ATNF pulsar database[2]. Data for pulsars in globular clusters were taken from the web-page[3] maintained by Paulo Freire, where the distances of the clusters and the DMs of pulsars are listed. The results from the original as well as from the modified NE2001 model are shown in Figure 1. Although there is a considerable scatter, the distances of pulsars estimated from the modified NE2001 model agree better with the observations than the original NE2001 model, especially for pulsars with distances larger than about 6 kpc.

We do not claim that our modified NE2001 model is a complete substitute for the NE2001 model in describing the diffuse ionized gas in the Galaxy. Other NE2001 components, such as the thin disk and the arm parameters, need to be correspondingly revised to properly interpret interstellar scattering and scintillation. A new model, NE2008, accounting for all new relevant observations is currently being developed (Jim Cordes, private communication).

[2] *http://www.atnf.csiro.au/research/pulsar/psrcat/*

[3] *http://www.naic.edu/~pfreire/GCpsr.html*

With the modified NE2001 thermal electron density model and the filling factors by Gaensler et al. (2008) as input, we simulated the all-sky free-free emission at 22.8 GHz. This is compared to the result by Sun et al. (2008) based on the original NE2001 model and the filling factors by Berkhuijsen et al. (2006). The WMAP five-year MEM thermal emission template (Gold et al. 2009) is shown for

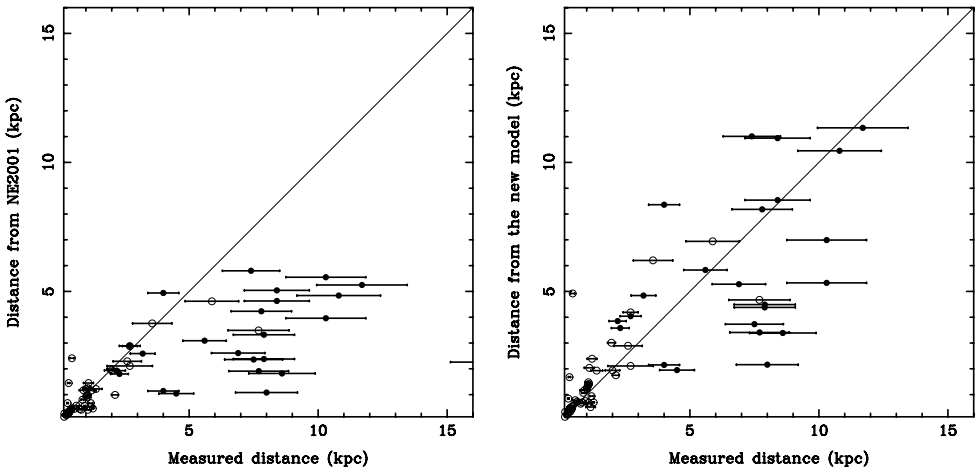

Fig. 1 Measured distances versus distance estimates from the NE2001 model (*left panel*) and the modified NE2001 model (*right panel*). The measurements from parallaxes are indicated by open circles and those from the associated globular clusters by filled circles. The lines mark the case where the measured and estimated distances are equal.

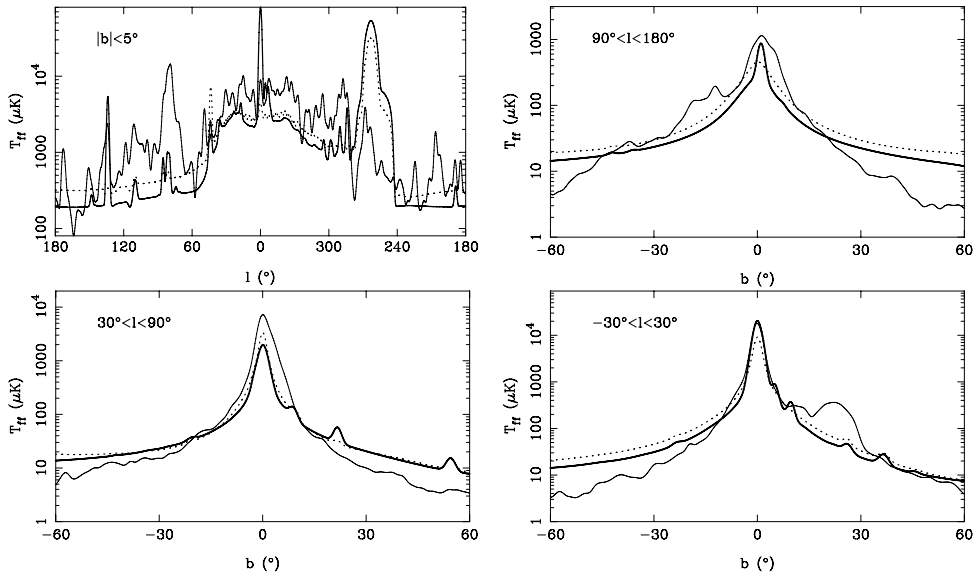

Fig. 2 Longitude and latitude profiles from the simulated and the template free-free emission maps at 22.8 GHz. The thin solid lines are from the WMAP five-year MEM template, the thick solid lines from the modified NE2001 model with the filling factors by Gaensler et al. (2008), and the dotted lines from the original NE2001 model with filling factors derived by Berkhuijsen et al. (2006).

comparison. Slices extracted from the above mentioned maps are shown in Figure 2. Note that the lower envelope of the observed emission is to be compared with the simulated profiles, which do not include all individual H II regions nor other local features. Along the Galactic plane, thermal emission from the modified NE2001 model is lower than that used by Sun et al. (2008), but still agrees with the observations. The reduction of thermal emission results from the smaller mid-plane electron density of 0.014 cm^{-3} in the modified model and 0.034 cm^{-3} in the NE2001 model.

The revised scale height by Gaensler et al. (2008) was not accepted everywhere. Savage & Wakker (2009) used the same data as Gaensler et al. (2008), but invoked a different fitting scheme, where an adjustable patchiness error was included to assure that $\chi^2_\nu \sim 1$. The fit by Gaensler et al. (2008) yielded $\chi^2_\nu \sim 5$. Savage & Wakker (2009) obtained a scale-height of about 1.4 kpc instead of 1.8 kpc by Gaensler et al. (2008). Their corresponding mid-plane density is then about 0.016 cm^{-3}. We ran simulations by modifying the thick disk components of the NE2001 model with the values by Savage & Wakker (2009), and found that the results do not vary significantly from those with a scale-height of 1.8 kpc, which we presented above. New pulsar data recently became available, which are also almost consistent with the 1.8 kpc scale-height, when applying the fitting method used by Savage & Wakker (2009) (Bryan Gaensler, private communication).

3.2 Regular Magnetic Field Properties

It is a customary to split the regular Galactic magnetic field into a disk and a halo component. The configurations of the disk fields were usually classified into three types: (1) axi-symmetric spiral (ASS); (2) bi-symmetric spiral (BSS); (3) following the spiral arms. The commonly used halo field patterns are toroidal, poloidal and a combination of both. The disk and halo fields and in particular their directions were mainly constrained by observed RMs.

3.2.1 The disk field

Early models for the disk magnetic field frequently used to study the propagation of ultrahigh energy cosmic-rays do not agree with the RMs observed from extragalactic sources (Sun et al. 2008) or from pulsars (Noutsos et al. 2008). Sun et al. (2008) have proposed three new models for the disk magnetic field configuration: ASS+RING with reversals in the Galactocentric rings, BSS, and ASS+ARM with reversals in the arms. All models predict RMs consistent with the available data. Reversals of the large-scale magnetic field have been a subject of a controversial debate for a long time. Recently, Nota & Katgert (2010) concluded that the magnetic field in the fourth Galactic quadrant exhibits reversals at the arm-interarm interfaces, which confirmed the earlier results obtained by Han et al. (2006). However, given the uncertain distances of pulsars and the difficulties in properly assessing the influence of foreground structures, such as H II regions, supernova remnants, Faraday Screens or the giant local loops, this topic clearly needs further investigations.

Here we kept the disk field of the SRWE08 models unchanged and simulated the RM map with the ASS+RING model as an example, which was recently further supported by new RM measurements (van Eck & Brown 2009). The RM profile along the Galactic plane taken from the maps is compared to the binned CGPS and SGPS RM data (Fig. 3: upper-left panel). The RM profile based on the modified NE2001 model and the ASS+RING disk field basically reproduce all the observed features. In general, the RM magnitudes from the present model are smaller than those modeled by Sun et al. (2008). For example, the RM gradient in the range of $80^\circ \leq l \leq 150^\circ$ is now more shallow than before. To reach an agreement between the updated and the SRWE08 models, we need to increase either the disk magnetic field strength or the thermal electron density. The local field strength of about 2 μG is determined by the RM/DM ratio of pulsars (e.g. Han et al. 2006). Beck et al. (2003) pointed out that the estimate of magnetic field strength by the RM/DM ratio is biased if there exists a correlation between the thermal electron density and the magnetic field strength. However,

Wu et al. (2009) performed simulations which showed that the RM/DM ratio correctly represents the mean strength of the magnetic field. Although there remain uncertainties on the turbulent properties of the interstellar medium, we consider the 2 μG local field strength to be very robust. Increasing the mid-plane thermal electron density by about a factor of two is about the same as in the NE2001 model and the RM profile from the present model is consistent with that from the SRWE08 model. However, the $\mathrm{DM}\sin|b|$ versus z could not be fitted well with the larger mid-plane electron density and a scale-height of 1.8 kpc. Possibly, the exponential description of the thermal electron density

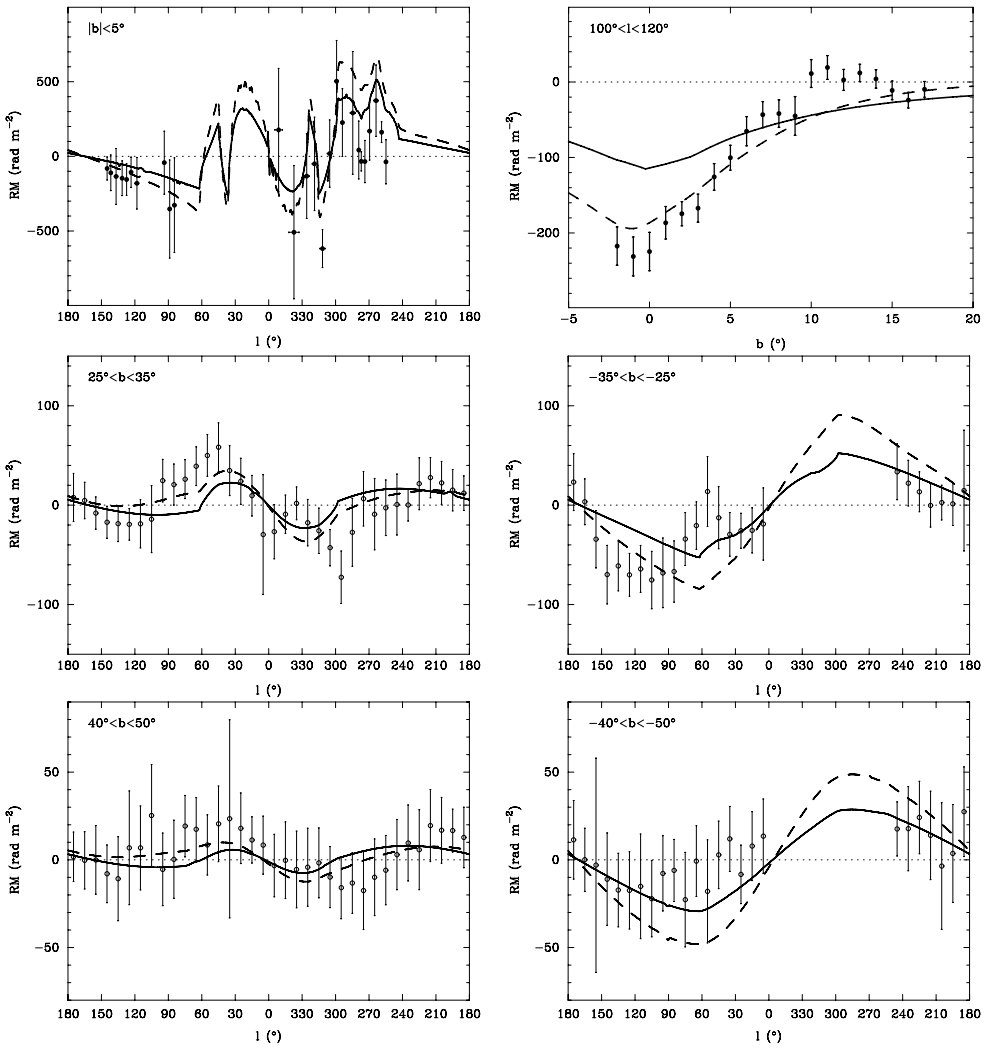

Fig. 3 RM profiles along Galactic longitudes and latitudes. The solid lines are from the present ASS+RING model, and the dashed lines from the corresponding SRWE08 model. The RMs in the plane (*upper-left* panel) are from the CGPS and SGPS (Brown et al. 2003, 2007). RMs in the area $100^\circ < l < 120^\circ$ and $-5^\circ < b < 20^\circ$ (*upper-right* panel) are from the CGPS extension (Jo-Anne Brown, in prep.), and in the halo regions from NVSS sources (Taylor et al. 2009).

is oversimplified or an additional electron density component exists, which just contributes near the plane. We anticipate that this point will be solved by the expected NE2008 model.

3.2.2 The halo field

The asymmetric distribution of RMs in longitude and latitude relative to the Galactic plane and the Galactic center indicates that the Galactic halo field has opposite signs below and above the plane. Sun et al. (2008) have described the toroidal halo field $B_\phi(R, z)$, following Prouza & Šmída (2003), by

$$B_\phi(R, z) = \mathrm{sign(z)} B_0 \frac{1}{1 + \left(\frac{|z| - z_0}{z_1} \right)^2} \frac{R}{R_0} \exp\left(-\frac{R - R_0}{R_0} \right), \quad (1)$$

where $\mathrm{sign}(z)$ takes the sign of z.

To account for the revised thermal electron density model, we obtained new parameters for the halo field as: $z_0 = 1.5$ kpc, $z_1 = 0.2$ kpc for $|z| < z_0$ and otherwise $z_1 = 4$ kpc, $B_0 = 2$ μG, and $R_0 = 4$ kpc. From new all-sky simulations with added halo and disk magnetic fields, we obtained the RM latitude profile for the longitude range of $100^\circ < l < 120^\circ$ (Fig. 3: the upper-right panel) to be compared with RM data from the CGPS high-latitude extension (Brown et al., in prep.). Near the Galactic plane, the simulated RM profile does not agree with the observations, which again is caused by the mid-plane thermal electron density being too small in our modified NE2001 model. The deviations vanish by increasing the thermal electron density by a factor of two as mentioned in Section 3.2.1 to reconcile the RM difference in the plane.

We also obtained average RM longitude profiles and show them for $25^\circ < b < 35^\circ$ and $40^\circ < b < 50^\circ$, as well as their southern counterparts in Figure 3 (middle and lower panels). These profiles were compared with the RMs from NVSS sources (Taylor et al. 2009) binned in 10° longitude intervals. RM profiles from new simulations generally reproduce the observed RM anti-symmetry with smaller amplitudes compared to the SRWE08 models.

There is evidence based on polarization data from the Global Magneto-Ionic Medium Survey (GMIMS)[4], currently running at the DRAO 26-m telescope at L-band (Wolleben et al. 2009, 2010b), that magnetized filaments are associated with a very local and therefore very extended H I shell located above the Galactic plane in the direction of the Galactic center with large positive and negative RMs in the first and forth quadrant, respectively (Wolleben et al. 2010a). Very likely, this bubble explains the RM deviations between the current halo model and the RM measurements seen in Figure 3 for the area $30^\circ < l < 60^\circ$ and $25^\circ < b < 35^\circ$. This finding does not question the present halo model, as its asymmetry above the plane of 10–20 rad m^{-2} is smaller than that attributed to the magnetized filaments. In the region $45^\circ < l < 60^\circ$ and $-60^\circ < b < -20^\circ$, Taylor et al. (2009) derived positive RMs for distinct small areas (see their fig. 4), which partly cancel the generally negative RMs in this area and cause deviations between simulations and observations. These small areas with positive RMs may be associated with southern Loop I filaments.

It is important to keep in mind that we observe the halo magnetic field in superposition with the disk field. Because the toroidal magnetic field above the plane is directed opposite to the disk field, the intrinsic RM asymmetry from the halo model is reduced. Vice versa, below the plane disk and halo field, the halo asymmetry becomes more evident (Fig. 3). It is therefore very important to obtain a large set of RM data for the southern sky, especially for the region of $240^\circ < l < 360^\circ$, to demonstrate that the predicted halo RM asymmetry exists. We note that the northern sky area with large negative RMs within $60^\circ < l < 140^\circ$ below the Galactic plane towards $b \sim -40^\circ$, named region A by Simard-Normandin & Kronberg (1980), might be influenced by Loop II, which is generally believed to be a local shell structure.

[4] *https://www.astrosci.ca/users/drao/gmims*

Nagar & Matulich (2009) suggested that a vertical field component needs to be added to the SRWE08 models to better describe deflections of ultrahigh energy cosmic-rays. This vertical field component has a strength of about 0.2 μG at the solar position, consistent with that derived by Han & Qiao (1994). We performed simulations including a vertical field of that strength as proposed by Prouza & Šmída (2003) and found the results just marginally deviate from the simulations without this component. This means that such a weak vertical field cannot be constrained by our simulations. Recently, Mao et al. (2010) obtained RMs of numerous extragalactic sources towards the northern and southern Galactic pole and convincingly demonstrated that there does not exist a coherent vertical field at the Sun's position. Therefore, we do not include any vertical magnetic field component in our models.

3.3 Random Magnetic Fields and the Cosmic-ray Electron Density

3.3.1 The random magnetic field component

Sun et al. (2008) and Sun & Reich (2009) have invoked isotropic random magnetic fields with a Gaussian distribution to simulate all-sky maps. Simulations of high angular resolution patches of the sky follow a power-law spectrum. Jaffe et al. (2010) have included an additional magnetic field component, called an "ordered" component, which is a regular field with numerous small-scale field reversals. Unlike isotropic random fields, this component contributes to total and polarized emission, which in turn reduces the cosmic-ray electron density to match observations. The "ordered" magnetic field does not increase a RM, but increases its scatter. Although this "ordered" component is clearly helpful to reach consistency between simulations and observations, the spatial scales of its reversals are entirely unclear and there is absolutely no evidence so far of its existence in our Galaxy. We therefore do not include an "ordered" component in our simulations.

3.3.2 The cosmic-ray electron density distribution

The SRWE08 models truncated the distribution of the cosmic-ray electron density at $|z| = 1$ kpc to avoid excessive synchrotron emission at high latitudes caused by the strong halo magnetic field. This truncation is certainly physically unrealistic. Since the halo magnetic field in the revised models is much smaller, this cutoff in z is not needed any more. A scale-height of 0.8 kpc instead of 1 kpc used by Sun et al. (2008) was found to adapt better to the data.

With the revised models, we simulated an all-sky total intensity map at 408 MHz and a polarized intensity map at 22.8 GHz at an angular resolution of $15'$. The 408 MHz map was then smoothed to $51'$, which is the angular resolution of the 408 MHz all-sky survey by Haslam et al. (1982). The simulated as well as the WMAP 22.8 GHz polarization maps (Hinshaw et al. 2009) were smoothed to 2° to increase the signal-to-noise ratio. Slices extracted from the simulated maps are shown in Figure 4 for 408 MHz total intensities and in Figure 5 for 22.8 GHz polarized intensities. The new simulations qualitatively agree with the observations at a level comparable to the SRWE08 models.

3.3.3 The local enhancement

The SRWE08 models include a local emission excess, realized by enhanced cosmic-ray electrons within 1 kpc, to account for the increase of the synchrotron emissivity towards the solar system based on low-frequency absorption data from optically thick H II regions. Clearly, the available data are quite limited and not suited to map the local synchrotron excess in 3D. The spherical approach used in the SRWE08 models is therefore almost arbitrary. It will be the task of LOFAR or other new low-frequency telescopes under construction to observe many more faint H II regions across the sky in order to model the local synchrotron excess in 3D. This task is closely related to obtaining a realistic halo model since both components are present at high latitudes. We note from Figure 4 that

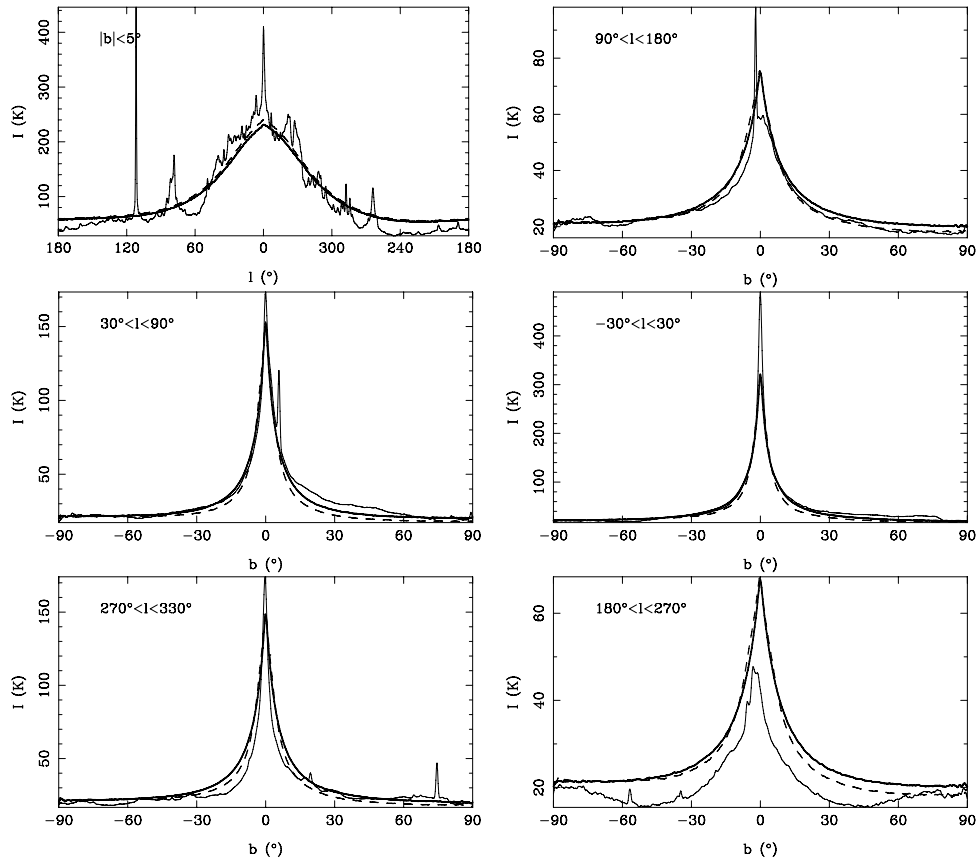

Fig. 4 Total intensity profiles at 408 MHz. The thin solid lines show profiles obtained from the 408 MHz all-sky total intensity survey (Haslam et al. 1982). The results from the new model and the SRWE08 model are displayed as thick solid and dashed lines, respectively.

for the region $180^\circ < l < 270^\circ$, the observed 408 MHz total intensity at high latitudes is below that expected from the simulations. This indicates a possible offset of the local excess center from the solar position. We shifted the center of the local enhancement towards $l = 45^\circ$, $b = 0^\circ$ with a distance of about 560 pc from the Sun and repeated our simulations. The results are shown in Figure 6. Quite obviously a much better agreement between the simulation and the observations is achieved by shifting the center of the local enhancement. However, there are not yet clues from observations on the center location and the 3D geometry of the local enhancements, so we are looking forward to numerous H II region absorption results obtained by LOFAR.

4 SUMMARY

In this paper, we updated the parameters of the 3D-emissivity models used by Sun et al. (2008) for all-sky simulations based on a revised thermal electron density scale-height by Gaensler et al. (2008). The scale-height and mid-plane electron density of the NE2001 thermal electron density model of 1 kpc and 0.034 cm^{-3} were replaced by 1.8 kpc and 0.014 cm^{-3}. As a consequence, the maximum halo field strength of 2 μG, and a scale-height of the cosmic-ray electron density of 0.8 kpc are obtained, which we consider to be much more physically relevant than the 10 μG field strength and

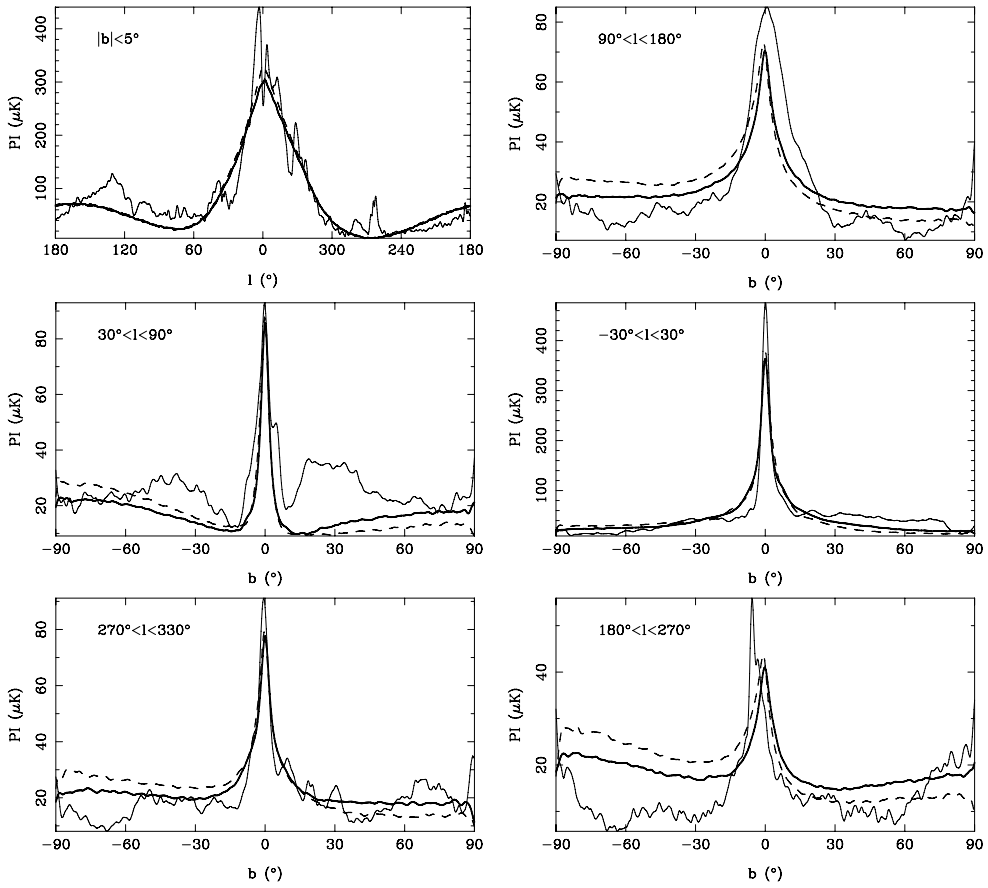

Fig. 5 Profiles as in Fig. 4, but for 22.8 GHz polarized intensities from the WMAP five-year data (Hinshaw et al. 2009).

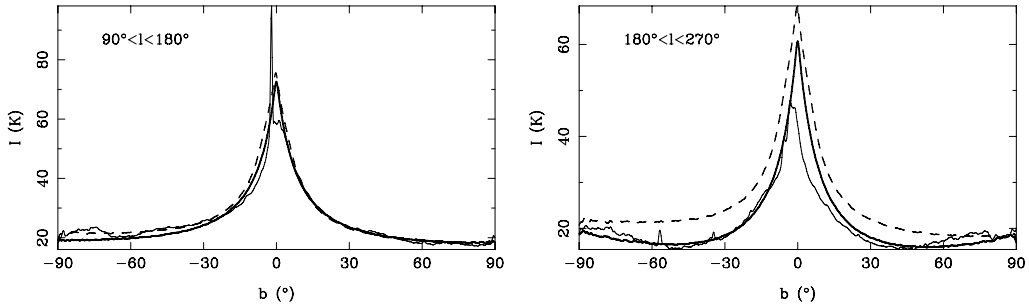

Fig. 6 Total intensity latitude profiles. The thin lines are from the 408 MHz all-sky survey. The solid lines are from the simulations with the local enhancement shifting by about 560 pc from the Sun, and the dashed lines are from the SRWE08 model.

the truncation with z at 1 kpc obtained by Sun et al. (2008). With these modifications, we reproduce the high latitude RM distribution of extragalactic sources, total intensity and polarized intensity all-sky survey maps in the same way as Sun et al. (2008). We note that the mid-plane thermal electron density needs to be increased by a factor of about two to properly represent the RMs in the Galactic plane. We also find that a shift of the center of the local synchrotron enhancement from the Sun's position by 560 pc towards $l = 45°$, $b = 0°$ significantly improves the models to adapt to total intensity observations towards the outer Galaxy.

Acknowledgements X. H. Sun acknowledges financial support by the MPG. He is grateful to Prof. M. Kramer for hospitality at the MPIfR and for financial support. We would like to thank Patricia Reich and Rainer Beck for thorough reading of the manuscript and helpful discussions.

References

Beck, R., Shukurov, A., Sokoloff, D., & Wielebinski, R. 2003, A&A, 411, 99
Berkhuijsen, E. M., Mitra, D., & Müller, P. 2006, AN, 327, 82
Berkhuijsen, E. M., & Müller, P. 2008, A&A, 490, 179
Brown, J. C., Taylor, A. R., & Jackel, B. J. 2003, ApJS, 145, 213
Brown, J. C., Haverkorn, M., Gaensler, B. M., et al. 2007, ApJ, 663, 258
Condon, J. J., Cotton, W. D., Greisen, E. W., et al. 1998, AJ, 115, 1693
Cordes, J. M., & Lazio, T. J. W. 2002 (astro-ph/0207156)
Cordes, J. M., & Lazio, T. J. W. 2003 (astro-ph/0301598)
Gaensler, B. M., Madsen, G. J., Chatterjee, S., & Mao, S. A. 2008, PASA, 25, 184
Gold, B., Bennett, C. L., Hill, R. S., et al. 2009, ApJS, 180, 265
Han, J. L., Manchester, R. N., Berkhuijsen, E. M., & Beck, R. 1997, A&A, 322, 98
Han, J. L., Manchester, R. N., Lyne, A. G., Qiao, G. J., & van Straten, W. 2006, ApJ, 642, 868
Han, J. L., & Qiao, G. J. 1994, A&A, 288, 759
Haslam, C. G. T., Salter, C. J., Stoffel, H., & Wilson, W. E. 1982, A&AS, 47, 1
Hinshaw, G., Weiland, J. L., Hill, R. S., et al. 2009, ApJS, 180, 225
Jaffe, T. R., Leahy, J. P., Banday, A. J., et al. 2010, MNRAS, 401, 1013
Jansson, R., Farrar, G. R., Waelkens, A., & Enßlin, T. A. 2009, JCAP, 7, 21
Kramer, M., Bell, J. F., Manchester, R. N., et al. 2003, MNRAS, 342, 1299
Lorimer, D. R., Faulkner, A. J., Lyne, A. G., et al. 2006, MNRAS, 372, 777
Mao, S. A., Gaensler, B. M., Haverkorn, M., et al. 2010, ApJ, 714, 1170
Nagar, N. M., & Matulich, J. 2009, A&A, in press (arXiv:0912.2131)
Nota, T., & Katgert, P. 2010, A&A, 513, A65
Noutsos, A., Johnston, S., Kramer, M., & Karastergiou, A. 2008, MNRAS, 386, 1881
Prouza, M., & Šmída, R. 2003, A&A, 410, 1
Savage, B. D., & Wakker, B. P. 2009, ApJ, 702, 1472
Simard-Normandeau, M., & Kronberg, P. P., 1980, ApJ, 242, 74
Sun, X. H., & Reich, W. 2009, A&A, 507, 1087
Sun, X. H., Reich, W., Waelkens, A., & Enßlin, T. A. 2008, A&A, 477, 573
Taylor, A. R., Stil, J. M., & Sunstrum, C. 2009, ApJ, 702, 1230
van Eck, C., & Brown, J. C. 2009, Bulletin of the American Physical Society, abstract B.1005
Verbiest, J. P. W., Lorimer, D. R., & McLaughlin, M. A. 2010, MNRAS, 405, 564
Waelkens, A., Jaffe, T., Reinecke, M., Kitaura, F. S., & Enßlin, T. A. 2009, A&A, 495, 697
Wolleben, M., Landecker, T. L., Carretti, E., et al. 2009, in IAU Symp. 259, Cosmic Magnetic Fields: From Planets to Stars and Galaxies, eds. K. G. Strassmeier, A. G. Kosovichev, & J. E. Beckman, 89
Wolleben, M., Fletcher, A., Landecker, T. L., et al. 2010, ApJ, 724, L48
Wolleben, M., Landecker, T. L., Hovey, G. J., et al. 2010, AJ, 139, 1681
Wu, Q., Kim, J., Ryu, D., Cho, J., & Alexander, P. 2009, ApJ, 705, L86